COMPUTATION OF PROPAGATION PROPERTIES IN A LATERALLY INHOMOGENEOUS STRATIFIED MEDIUM: UNDERWATER TRANSMISSION

Angelos Amditis

National Technical University of Athens
Electrical and Computer Engineering
Microwaves and Optics Lab, Athens, Greece
e-mail: angelos@esd.ece.ntua.gr

Abstract

Propagation of acoustic waves generated from a source within a laterally inhomogeneous layered sea medium is examined using analytical techniques. A two-step analytical approach is employed. Starting from the computation of response function of the stratified medium, integral equation techniques are employed to analyze the case of inhomogeneous medium. The use of contour integration techniques allows the development of field expressions in terms of normal modes of the stratified sea medium with arbitrary number of layers. Field calculation is carried out for a sinusoidal lateral inhomogeneous sea medium. Numerical computations are carried out and the effects of inhomogeneites are examined.

1. INTRODUCTION

A commonly used model to analyze the propagation of acoustic waves inside the sea is the stratified medium characterized with individual salinity and temperature as shown in figure1.

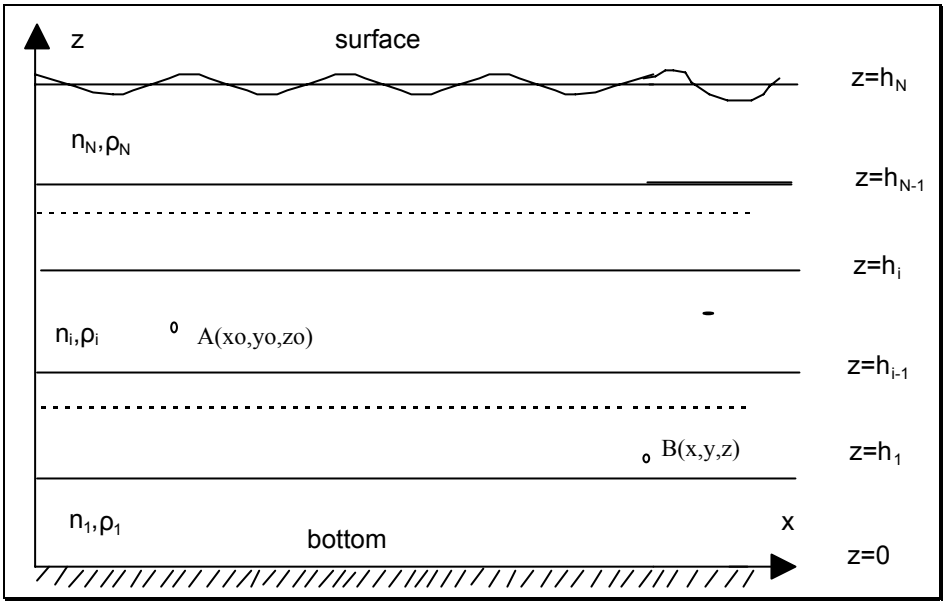

Figure 1. Stratified sea medium

Assuming the seabed and surface to be perfectly planar the propagation of acoustic waves emitted by a source could be treated using the separation of variables technique.

The analysis shows that the acoustic propagation in thin layered media is realized by normal modes associated with the guided waves between the layers. As the oscillation frequency increases there are large numbers of propagation modes thus leading into a highly dispersive transfer function between source and receiving points. Although the study of propagation in this type sea model is highly useful in many instances, there is a lateral variation within the layers constituting the sea. Therefore it is necessary to develop computational techniques coping with lateral inhomogeneites to determine the associated effects in underwater acoustics.

In figure 2 the acoustic model studied in this article is shown. The refractive index - velocity profile of the sea medium is described by the equation:

$$n(x,z) = n_0(z) + \Delta n \cos(\Omega_x x) = n_0(z) + \delta n(x,z) \tag{1}$$

where $n_0(z)$ is the horizontally stratified medium refractive index while the second term represents the disturbance because of the lateral inhomogeneity which is taken to be periodic.

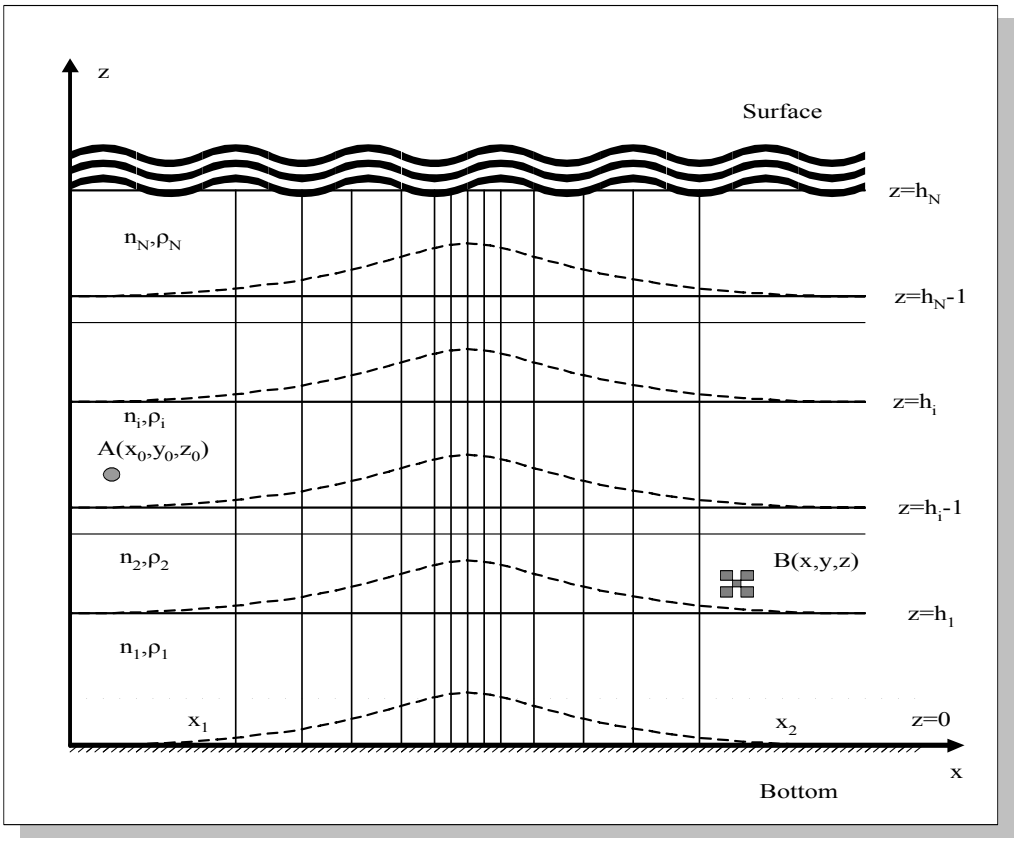

Figure 2. Inhomogeneous Sea medium

In equation (1) Ω_x is the angular frequency of the sinusoidal lateral inhomogeneity, having units of m^{-1} and defined as follows:

$$\Omega_x = \frac{2\pi}{2(x_2 - x_1)} \tag{2}$$

where x_1 and x_2 are the limits of the lateral sinusoidal disturbance as its shown in figure 2.

In the following, a two-step Green's function approach is applied to calculate the acoustic field inside the sea when an elementary source is oscillating at an arbitrary frequency ω. In the first instance the Green's function of the horizontally stratified medium is determined using the Sommerfeld technique. Then an integral equation is written to take into account the effects of the lateral inhomogeneity. This equation is solved approximately by computing the first order iteration. The corresponding integrals are calculated analytically up to some extend and then numerical integration techniques are employed.

2. INTEGRAL EQUATION TECHNIQUE

Consider an elementary continues wave source oscillating at angular frequency ω and placed at the point $\vec{r}_0$ as shown in figure 1. The pressure wave equation can be written as follows:

$$\left(\nabla^2 + n^2(x,z)k_0^2\right)\vec{G}\left(\vec{r},\vec{r}_0\right) = -\delta\left(\vec{r} - \vec{r}_0\right) \tag{3}$$

where k_0 is the reference wavenumber and $G(\vec{r},\vec{r}_0)$, is the pressure at the observation point $r(\vec{x},\vec{y},\vec{z})$. In writing equation (3) an $\exp(-j\omega t)$ time dependence is assumed silently.

If the medium is horizontally homogeneous (i.e. $\Delta n = 0$ in eq. (1)) then eq. (3) can be written as follows:

$$\left(\nabla^2 + n_0{}^2(z)k_0^2\right)\vec{G}_0\left(\vec{r},\vec{r}_0\right) = -\delta\left(\vec{r} - \vec{r}_0\right) \tag{4}$$

where $G_0(\vec{r},\vec{r}_0)$ represents the solution for this case.

In addition to eqs. (3) and (4), one has to take into account the boundary conditions associated with the sea surface, bottom and interface between the medium layers. Specifically at the sea-air interface the pressure is taken to be [1]:

$$P_S = 0 \tag{5}$$

while on the sea bottom the boundary condition is [2]:

$$\frac{\partial P_B}{\partial \vec{n}} = 0 \tag{6}$$

Furthermore at the interface of the layers in case of horizontally homogeneous medium the pressure wave and its normal derivative satisfy the conditions [3]:

$$P_1 = P_2 \quad \text{and} \quad \frac{1}{j\omega\rho_1}\frac{\partial P_1}{\partial \vec{n}} = \frac{1}{j\omega\rho_2}\frac{\partial P_2}{\partial \vec{n}} \tag{7}$$

respectively, where ρ_n is the medium density in the nth layer and ω is the acoustic source's angular frequency. Assuming the solution of eq. (4), $G_0(\vec{r},\vec{r}_0)$, subject to relevant boundary conditions (eq. (5)-(7)), is known, then by applying the Green's theorem, the following integral equation is derived:

$$\begin{aligned}\int_{V\infty}\left[G_0(\vec{r},\vec{r}\,')\nabla'^2 G(\vec{r}\,',\vec{r}_0) - G(\vec{r},\vec{r}\,')\nabla'^2 G_0(\vec{r}\,',\vec{r}_0)\right]dV' = \\ = -\int_{S\infty}\left[G_0(\vec{r},\vec{r}\,')\frac{\partial}{\partial \vec{n}'}G(\vec{r}_0,\vec{r}\,') - G(\vec{r}_0,\vec{r}\,')\frac{\partial}{\partial \vec{n}'}G_0(\vec{r}\,,\vec{r}\,')\right]dS'\end{aligned} \tag{8}$$

where V_∞ is the whole sea medium volume and S_∞ is the surface surrounding this volume (see fig.2). On substituting eqs. (3) and (4) into (8), taking into account the boundary conditions on the sea bottom and surface (eq. (5) and (7)), as well as the radiation condition for $x \to \pm\infty$ and $y \to \pm\infty$, eq.(8) results into:

$$\vec{G}(\vec{r},\vec{r}_0) = \vec{G}_0(\vec{r},\vec{r}_0) + \int_{V_\infty}\begin{bmatrix} -\vec{G}_0(\vec{r},\vec{r}\,')n_0^2(z')k_0^2\vec{G}(\vec{r}\,',\vec{r}_0) - \vec{G}_0(\vec{r},\vec{r}\,')\delta n(x',z')k_0^2\vec{G}(\vec{r}\,',\vec{r}_0) + \\ + \vec{G}(\vec{r},\vec{r}\,')n_0^2(z')k_0^2\vec{G}_0(\vec{r}\,',\vec{r}_0)\end{bmatrix}dV' \tag{9}$$

where $\vec{r}_0$ is the position vector of the acoustic source. Interpretation of eq. (9) shows that the pressure field at an arbitrary point $\vec{r}$ consists of a superposition of the field $G_0(\vec{r},\vec{r}_0)$, in the absence of horizontal inhomogeneity and a second term, which is associated to scattering phenomena because of the lateral disturbance of the refractive index.

A direct solution of eq.(9) is a highly difficult task, even if taking a simple refractive index disturbance like the following:

$$\delta n(x,z) = n^2(x,z) - n_0^2(z) \tag{10}$$

In case of weak disturbance ($(\delta n)^2 \langle\langle 1$), then eq. (9) could be solved approximately by using a first order iteration (Born Approximation), that is by substituting $G(\vec{r},\vec{r}_0)$ inside the integral with $G_0(\vec{r},\vec{r}_0)$ which leads to the following integral equation:

$$G(\vec{r},\vec{r}_0) = G_0(\vec{r},\vec{r}_0) + \int_{V\infty} \delta n(x',z') G_0(\vec{r},\vec{r}\,') G_0(\vec{r}\,',\vec{r}_0) dV' \tag{11}$$

and since in principle the integral in the right side of eq. (11) is computable the first approximation of the acoustic pressure field can be calculated.

It is evident that in order to use eq. (11), the $G_0(\vec{r},\vec{r}_0)$ function must be known accurately and in such a format that the three dimensional integral to be computed with minimum numerical cost. Therefore it is required to determine $G_0(\vec{r},\vec{r}_0)$ in a closed form. In the following section an outline of the method used to determine $G_0(\vec{r},\vec{r}_0)$ is presented.

3. COMPUTATION OF THE FIELD IN THE ABSENCE OF HORIZONTAL VARIANCE

A model structure shown in figure 1 is taken in order to analyze the wave propagation in a range independent sea medium. A layered medium is assumed where the refractive index is taken to be discrete valued while a three dimensional variation is assumed on the layers interface. A realistic three dimensional model of sea medium in terms of propagation characteristics is taken through this structure.

In order to treat the problem of calculating the acoustic field distribution originating from an elementary source at a point *A* (see figure 1), at an arbitrary point *B* having corresponding co-ordinates (x_0,y_0,z_0) and (x,y,z), respectively, a Green's function formulation is proposed. Then the Green's function for this medium is calculated using the standard separation of variables technique as described briefly in the following [4].

Assuming the elementary source point being inside the *i*th layer, the field inside the sea medium is obtained by taking into account the primary field generated from the elementary source and the secondary field induced inside each layer. The implementation of the Green's theory for an elementary source at a point $r_0(x_0,y_0,z_0)$ suggests that the Green's function at a point $r(x,y,z)$ represents the pressure field derived from the source at that point [5]. The Helmholtz equation satisfied within the source layer is written as follows [5]:

$$\left(\nabla^2 + n_i^2 k_i^2\right)\vec{G}_p\left(\vec{r}/\vec{r}_0\right) = -\delta\left(\vec{r}-\vec{r}_0\right) \quad , \quad n_i = c_0/c_i \quad , \quad k_0 = \omega/c_0 = 2\pi f_0/c_0 \tag{12}$$

where the $\vec{G}_p\left(\vec{r}/\vec{r}_0\right)$ function represents the primary field; n_i and c_i are the refractive index and the sound speed in the *i*th layer respectively; c_0 is the reference sound speed

and f_o is the acoustic source frequency. Furthermore the homogeneous Helmholtz equation satisfied in the other layers, is:

$$\left(\nabla^2 + n_n^2 k_n^2\right)\vec{G}_{sn}\left(\vec{r}/\vec{r}_0\right) = 0 \qquad , \qquad n = 1,\ldots,N \quad , \quad n \neq i \tag{13}$$

where $\vec{G}_{sn}\left(\vec{r}/\vec{r}_0\right)$ represents the secondary field in the nth layer and N is the layers number [6]. The composition of eqs (12) and (13) leads to the following general expression for the Green's function $\vec{G}_0\left(\vec{r}/\vec{r}_0\right)$:

$$\vec{G}_0\left(\vec{r}/\vec{r}_0\right) = \begin{cases} \vec{G}_p\left(\vec{r}/\vec{r}_0\right) + \vec{G}_{sn}\left(\vec{r}/\vec{r}_0\right) & , \quad n = i \\ \vec{G}_{sn}\left(\vec{r}/\vec{r}_0\right) & , \quad n \neq i \end{cases} \tag{14}$$

Applying the spatial Fourier transformation and after integration of the k_z-component the G_p and the G_{sn} functions are written as follows [7], [8]:

$$\vec{G}_p\left(\vec{r}/\vec{r}_0\right) = -\frac{1}{8\pi^2}\int_{-\infty}^{+\infty} dk_x \int_{-\infty}^{+\infty} dk_y \exp\left[jk_x\left(x - x_0\right) + jk_y\left(y - y_0\right)\right]\frac{\exp(\mu_i\left|z - z_0\right|)}{\mu_i} \tag{15}$$

$$\vec{G}_{sn}\left(\vec{r}/\vec{r}_0\right) = \frac{1}{(2\pi)^2}\int_{-\infty}^{+\infty} dk_x \int_{-\infty}^{+\infty} dk_y \exp\left[jk_x\left(x - x_0\right) + jk_y\left(y - y_0\right)\right]\begin{bmatrix} A_n\left(k_x, k_y\right)\exp\left(-\mu_n z\right) + \\ + B_n\left(k_x, k_y\right)\exp\left(\mu_n z\right) \end{bmatrix} \tag{16}$$

where $$\mu_n = \sqrt{k_x^{\ 2} + k_y^2 - k_0^2 n_n^2} \tag{17}$$

The calculation of the scalar coefficients A_n and B_n of eq.(16) is obtained from the application of the boundary conditions on the sea layers, surface, and bottom (eq. (5)-(7)).

The latter results into a recursive equation which includes all the information concerning the propagation model characteristics and is written as follows [9]:

$$M\left(n+1, n+1\right)m_{n+1} = M\left(n+1, n+2\right)m_{n+2} \qquad , \qquad m_n = \begin{bmatrix} A_n \\ B_n \end{bmatrix} \tag{18}$$

$$M\left(t,s\right) = \begin{bmatrix} \left(\frac{1}{2} + \frac{\rho_t \mu_s}{2\rho_s \mu_t}\right)\exp\left(-\mu_s h_t\right) & \left(\frac{1}{2} - \frac{\rho_t \mu_s}{2\rho_s \mu_t}\right)\exp\left(\mu_s h_t\right) \\ \left(\frac{1}{2} - \frac{\rho_t \mu_s}{2\rho_s \mu_t}\right)\exp\left(-\mu_s h_t\right) & \left(\frac{1}{2} + \frac{\rho_t \mu_s}{2\rho_s \mu_t}\right)\exp\left(\mu_s h_t\right) \end{bmatrix} \tag{19}$$

Equation (18) is valid for all the layers with the exception of the source layer. If the latter is the *i*th layer then it is bounded from the $z = h_{i-1}$ and $z = h_i$ surfaces (see figure1). The application of the boundary conditions on these two surfaces leads to the following equations:

$$M(i-1,i-1)m_{i-1} = M(i-1,i)m_i + n(i-1,i) \quad , \quad z = h_{i-1} \tag{20}$$

$$n(i,i) + M(i,i)m_i = M(i,i+1)m_{i+1} \quad , \quad z = h_i \tag{21}$$

where

$$n(t,s) = \begin{bmatrix} \frac{1}{2} - sign(h_t - z_0)\frac{\rho_t \mu_s}{2\rho_s \mu_t} \\ \frac{1}{2} + sign(h_t - z_0)\frac{\rho_t \mu_s}{2\rho_s \mu_t} \end{bmatrix} \frac{\exp(\mu_s |h_t - z_0|)}{8\pi^2 \mu_s} \tag{22}$$

where z_0 shows the source position on the *z*-axis and the $sign(h_t - z_0)$ function is defined as follows:

$$sign(h_t - z_0) = \begin{cases} +1 & , \quad h_t > z_0 \\ 0 & , \quad h_t = z_0 \\ -1 & , \quad h_t < z_0 \end{cases}$$

Following the calculation of A_n and B_n coefficients from eqs. (18),(20),(21) the Green's function is obtained from eqs.(15) and (16). The calculation of the integrals in eq.(16) has been carried out by means of Complex Contour Integration techniques. The above described method is leading to an expression for the Green's function and thus for the pressure field of an exponential form:

$$G_{sk} = \sum_{\ell=1}^{N_0} f_\ell(r) e^{-j\beta_\ell r} + \sum_{\ell=1}^{\infty} \phi_\ell(r) e^{-j\gamma_\ell r} \tag{23}$$

where the f_ℓ and the ϕ_ℓ represent the contribution of the different normal modes and evanescent modes respectively, to the pressure field, while the β_ℓ and the γ_ℓ are the real and imaginary poles of eq.(16) respectively and finally *r* is the range from the acoustic source [10].

In the above summation (eq. 23) the propagating modes are of finite number while an infinite number of evanescent waves are encountered, having a purely imaginary propagation number. The latter exhibits a series with highly convergent rate.

These non-propagating modes represent the energy stored in the vicinity of the acoustic source.

4. COMPUTATION OF GREEN'S FUNCTION IN CASE OF A LATERALLY INHOMOGENEITY

In order to compute the Green's function in case of a sinusoidal lateral inhomogeneity the $G_0(\vec{r},\vec{r}_0)$ function, in the format determined in the previous section, is substituted into eq. (11). Then after a lengthy procedure based on the following steps the $G(\vec{r},\vec{r}_0)$ function is computed. These steps are:

a) The $G_0(\vec{r},\vec{r}_0)$ Green's function is expressed in terms of it's Fourier representation and is substituted into eq.(11) resulting into [11] :

$$\vec{G}\left(\vec{r}/\vec{r}_0\right)=\vec{G}_0\left(\vec{r}/\vec{r}_0\right)+\frac{k_0^2}{(2\pi)^4}\int_{x_1}^{x_2}dx'\int_{-\infty}^{+\infty}dy'\int_0^h dz'\left\{\begin{array}{l}\left[\int_{-\infty}^{+\infty}dk_x\int_{-\infty}^{+\infty}dk_y e_1(k_x,k_y)Q_1(k_x,k_y)\right]\cdot\\ \cdot\left[\int_{-\infty}^{+\infty}dk'_x\int_{-\infty}^{+\infty}dk'_y e_2(k'_x,k'_y)Q_2(k'_x,k'_y)\right]\end{array}\right\}\Delta n\cos\Omega_x x' \tag{24}$$

where

$$e_1(k_x,k_y)=\exp[jk_x(x-x')+jk_y(y-y')] \tag{25a}$$

$$e_2(k'_x,k'_y)=\exp[jk'_x(x'-x_0)+jk'_y(y'-y_0)] \tag{25b}$$

$$Q_1(k_x,k_y)=A_n(k_x,k_y)\cdot\exp[-\mu_n(k_x,k_y)\cdot z]+B_n(k_x,k_y)\cdot\exp[\mu_n(k_x,k_y)\cdot z] \tag{25c}$$

$$Q_2(k'_x,k'_y)=A_n(k'_x,k'_y)\cdot\exp[-\mu_n(k'_x,k'_y)\cdot z']+B_n(k'_x,k'_y)\cdot\exp[\mu_n(k'_x,k'_y)\cdot z'] \tag{25d}$$

b) The definite x', y' and z' integrals appearing in eq.(24) are computed analytically by using the indefinite integrals [12]:

$$\int e^{\alpha x}\cos(bx)dx=\frac{e^{\alpha x}[a\cos(bx)+b\sin(bx)]}{a^2+b^2} \tag{26a}$$

$$\int e^{ax}dx=\frac{e^{ax}}{a} \tag{26b}$$

and the definite integral [12]:

$$\frac{1}{2\pi}\int_{-\infty}^{+\infty}e^{jax}dx=\delta(a) \tag{26c}$$

c) A $\delta\left(k_y' - k_y\right)$ behavior is obtained because of the homogeneity of the sea medium with respect to the y axis, thus the resulting four dimensional integrals are reduced to three dimensions.

These three dimensional spectral domain integrals, resulting, from the previous steps, have the general form :

$$\int_{-\infty}^{+\infty} dk_y e^{jk_y(y-y_0)} \int_{-\infty}^{+\infty} dk_x e^{jk_x(x-x_i)} e^{-\mu_n(k_x,k_y)\cdot z} \frac{Q(k_x,k_y)}{P(k_x,k_y)} \int_{-\infty}^{+\infty} dk_x' \frac{k_x' e^{jk_x'(x_i-x')}}{\mu_n(k_x',k_y)\left[\Omega_x{}^2 - \left(k_x' - k_x\right)^2\right]} \frac{Q(k_x',k_y)}{P(k_x',k_y)} \tag{27}$$

where

$x_i = x_1 \quad or \quad x_2$ (see fig.1)

Ω_x is the disturbance frequency (see eq.2)

Q/P are the Green's function Fourier transformation coefficients (A_n or B_n)

μ_n is defined with eq.16

d) The next step involves the computation of the k_x' integral of eq. (27), which is performed by using Complex Contour Integration techniques. As already mentioned the poles on the imaginary axis have diminishing contribution at the far field and therefore are neglected in computing the received field. Thus on computing the residue contribution of the real poles, the field strength is computed. These real poles include the N poles of the $G_0(\vec{r},\vec{r}_0)$ Green's function (see section 3), plus two other poles resulting from the term $(\Omega_x^2 - (k_x' - k_x)^2)$ of eq.(27). Specifically the real poles of the k_x' integral are:

$$\begin{aligned} &\lambda_k, \quad k = 1, N \\ &\lambda_{N+1} = k_x + \Omega_x \\ &\lambda_{N+2} = k_x - \Omega_x \end{aligned} \tag{28}$$

e) The remaining two integrals with respect to the k_x and k_y variables are transformed from spectral to polar coordinates as follows:

$$\begin{aligned} k_x &= \lambda \cos\varphi_\lambda \\ k_y &= \lambda \sin\varphi_\lambda \end{aligned} \tag{29}$$

Furthermore the spatial coordinates describing the relative source-receiver positions are also expressed in terms of spherical coordinates:

$$\begin{aligned} \rho &= R\cos\Psi \\ z &= R\sin\Psi \end{aligned} \tag{30}$$

At the same time the x and y variables appearing at eq. (27) are expressed in terms of polar coordinates:

$$\begin{aligned} x &= \rho\cos\varphi \\ y &= \rho\sin\varphi \end{aligned} \tag{31}$$

Considering the oscillatory behavior of the exponential terms resulting from the above transformations, which have the form:

$$\exp[R(j\cos\Psi\cos(\varphi-\varphi_\lambda)+\mu_n\sin\Psi)] \tag{32}$$

when $R\to+\infty$ the λ - integration is carried out by applying the stationary phase technique [13]. Thus the result is obtained by using the stationary phase formula

$$f(x)=\int_a^b e^{jxh(\lambda)}g(\lambda)d\lambda \cong g(\lambda_{sp})\left[\frac{2\pi}{x\left|h''(\lambda_{sp})\right|}\right]^{1/2}\exp\left[j(xh(\lambda_{sp})\pm\frac{\pi}{4})\right] \tag{33}$$

where λ_{sp} are the roots of the equation $h'(\lambda)=0$, while $h'(\lambda)$ and $h''(\lambda)$ are standing for the first and the second derivative of the $h(\lambda)$ function respectively. The sign in the exponential of the eq. (33) depends on the sign of the $h''(\lambda_{sp})$ function. Specifically it is plus for a positive value, while it is minus for a negative value of $h''(\lambda_{sp})$.

The ultimate result is computed in the following form (see eq. 11)

$$G(\vec{r},\vec{r}_0)=G_0(\vec{r},\vec{r}_0)+\delta p(\vec{r},\vec{r}_0) \tag{34}$$

where $\delta p(\vec{r},\vec{r}_0)$ is the resulting one dimensional integral, having the general form

$$\delta p(\vec{r},\vec{r}_0)=\sum_{i=1}^{48}\left[\int_0^\pi d\varphi_\lambda f_i(R,\varphi_\lambda)\right] \tag{35}$$

where

$$f_i(R,\varphi_\lambda)=\sum_{k=1}^{3}F_k(R,\varphi_\lambda) \tag{36}$$

At equation (36) $F_k(R,\varphi_\lambda)$ are the resulting functions from the above described procedure (steps a-e), having the following formulation:

$$F_1(R,\varphi_\lambda) = -k_n^2 e^{\pm j\frac{\pi}{4}} \cdot C(\lambda_{sp}) \cdot E_1(\varphi_\lambda) \cdot L(\varphi_\lambda) \cdot e^{d_1(\varphi_\lambda)}$$

$$F_2(R,\varphi_\lambda) = \frac{j\pi k_n^3 e^{\pm j\frac{\pi}{4}}}{\mu_n(\lambda_{N+1}) \cdot \Omega_x} \cdot \frac{Q^2(\lambda_{sp})}{P(\lambda_{sp}) \cdot P(\lambda_{N+1})} \cdot E_2(\varphi_\lambda) \cdot L(\varphi_\lambda) \cdot e^{d_2(\varphi_\lambda)} \tag{37}$$

$$F_3(R,\varphi_\lambda) = -\frac{j\pi k_n^3 e^{\pm j\frac{\pi}{4}}}{\mu_n(\lambda_{N+2}) \cdot \Omega_x} \cdot \frac{Q^2(\lambda_{sp})}{P(\lambda_{sp}) \cdot P(\lambda_{N+2})} \cdot E_2(\varphi_\lambda) \cdot L(\varphi_\lambda) \cdot e^{d_2(\varphi_\lambda)}$$

where

$$C(\lambda_{sp},\varphi_\lambda) = j2\pi \frac{Q(\lambda_{sp})}{P(\lambda_{sp})} \sum_{k=1}^{N} \frac{\lambda_k \cdot e^{j\lambda_k x_i} Q(\lambda_k)}{\mu_n(\lambda_k) \cdot \left[\Omega_x^2 - (k'_{xk} - \lambda_{sp}\cos\varphi_\lambda)^2\right] \cdot P'(\lambda_k)}$$

$$E_1(\varphi_\lambda) = \frac{\tan\Psi \cdot \cos(\varphi - \varphi_\lambda)}{\cos^2(\varphi - \varphi_\lambda) + \tan^2\Psi}$$

$$E_2(\varphi_\lambda) = E_1(\varphi_\lambda) \cdot \frac{\cos(\varphi - \varphi_\lambda) \cdot \cos\varphi_\lambda}{\left[\cos^2(\varphi - \varphi_\lambda) + \tan^2\Psi\right]^{1/2}} \tag{38}$$

$$L(\varphi_\lambda) = \left[\frac{2\pi\left[\cos^2(\varphi - \varphi_\lambda) + \tan^2\Psi\right]^{1/2}}{k_n R\left|-\cos\Psi \cdot \cos^2(\varphi - \varphi_\lambda) - \tan\Psi \cdot \sin\Psi\right|}\right]^{1/2}$$

$$d_1(\varphi_\lambda) = jk_n \frac{\cos(\varphi - \varphi_\lambda) \cdot \cos\varphi_\lambda x_i + R \cdot \cos\Psi \cdot \cos^2(\varphi - \varphi_\lambda) + R \cdot \tan\Psi \cdot \sin\Psi}{\left[\cos^2(\varphi - \varphi_\lambda) + \tan^2\Psi\right]^{1/2}}$$

$$d_2(\varphi_\lambda) = jk_n R \frac{\cos\Psi \cdot \cos^2(\varphi - \varphi_\lambda) + \tan\Psi \cdot \sin\Psi}{\left[\cos^2(\varphi - \varphi_\lambda) + \tan^2\Psi\right]^{1/2}}$$

The final integration of eq. (35) is carried out by means of numerical integration techniques, and specifically by applying the Simpson numerical integration technique [14].

5. NUMERICAL COMPUTATIONS

Numerical computations have been carried out for several cases of sea layer distributions while real data from different places of the Aegean sea have been used for the model characteristics. The frequency region of *1-1000 Hz* with emphasis to frequencies up to *200 Hz* was used while there were no limitations to range properties.

The examples that are presented here are referred to a specific area of the Aegean Sea with known acoustic medium characteristics having a depth of 281 m. In figure 3 the sound speed and the medium's density profiles are presented for the specific area.

As it can be observed from figure 3 the sound speed profile includes sharp changes especially near the surface leading to a very complex sound propagation medium. Noticeable changes are also being observed and at the density profile in the same figure.

Taking into account the above specific profiles the medium is divided into seven layers in order to simulate as well as possible its acoustic characteristics. The result is shown in figure 4.

For this specific environment numerical calculations have been carried out for different frequencies, source and receiver positions as well as for both the cases of the range independent and range dependent medium with interesting results.

Figure 3. Sound speed and density profiles

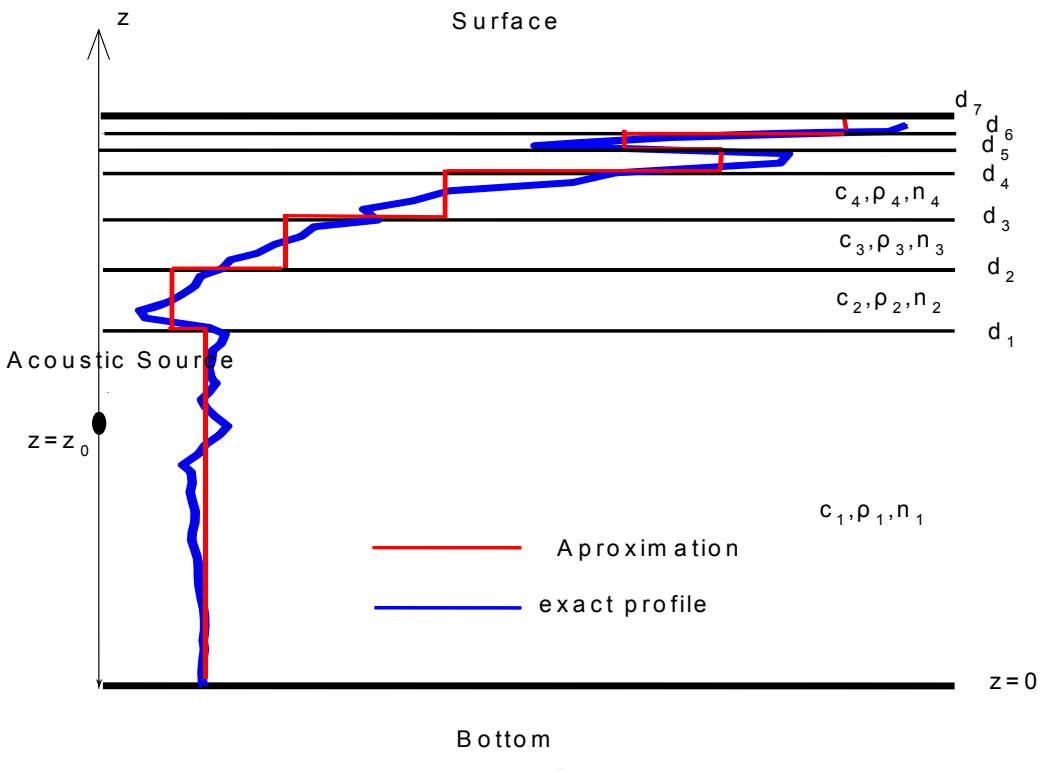

Figure 4

At the next group of figures the differences at the pressure filed because of the inserted disturbance (see figure 2) will be examined. This difference P_{diff} is expressed in dB.

These figures are related with a disturbance having as dimensions $x_1 = 10\ Km$ και $x_2 = 30\ Km$ (see figure 2). These dimensions are satisfying also the assumption for very large x_1 και x_2. The amplitude of the disturbance was calculated in relation with the change of the refractive index at the layers separation surfaces. It is obvious that Δn should be at least one order of value smaller than the differences between the values of the refractive index of successive layers.

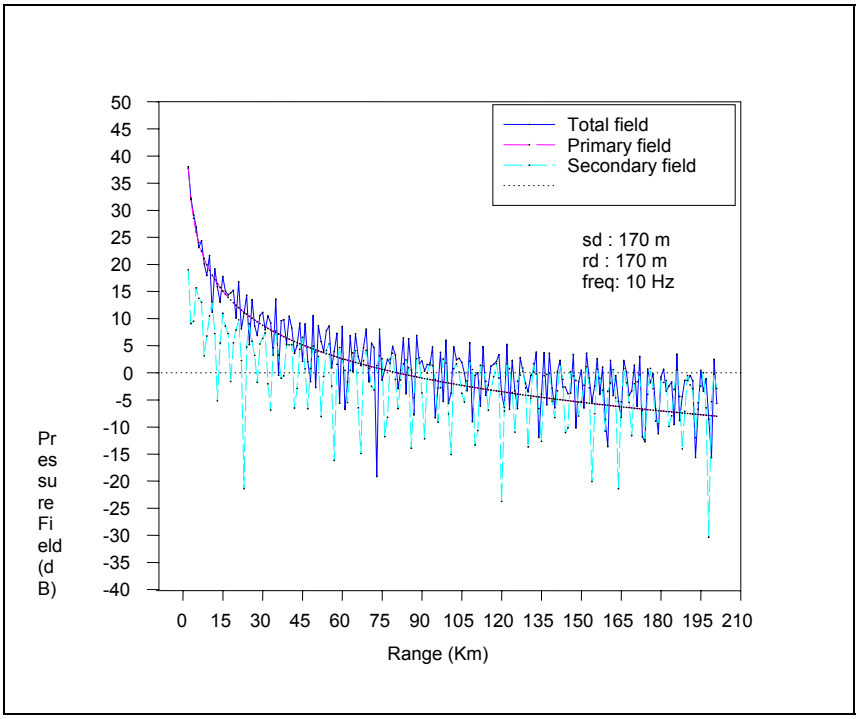

Figure 5. Acoustic field versus distance for a frequency of 10 Hz.

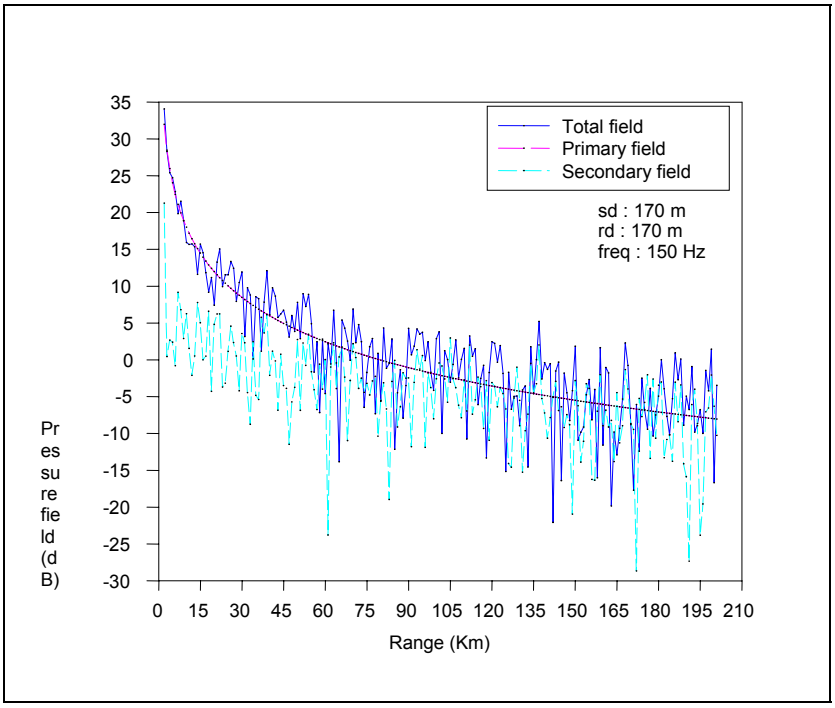

Figure 6. Acoustic field versus distance for a frequency of 150 Hz.

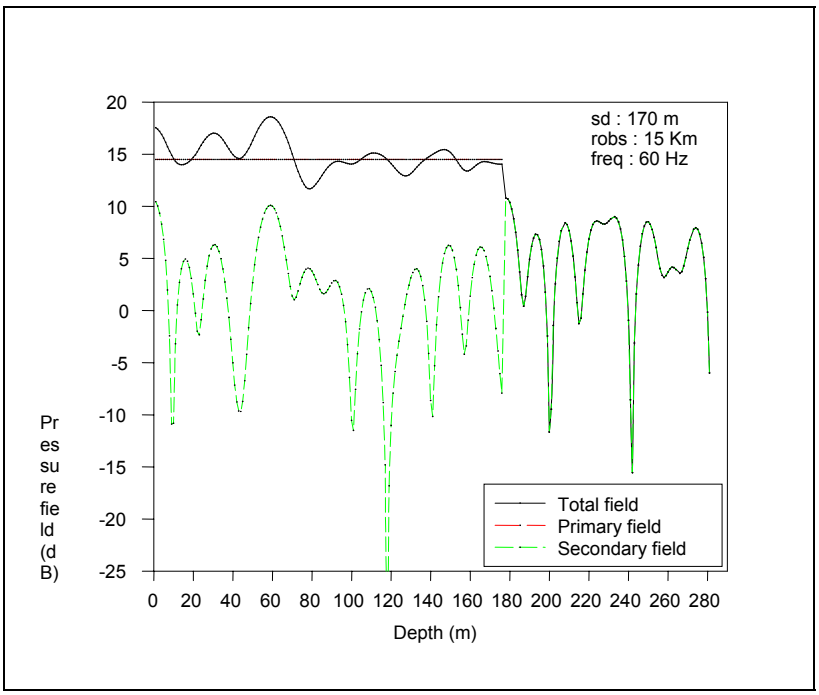

Figure 7. Acoustic field versus depth for a frequency of 60 Hz.

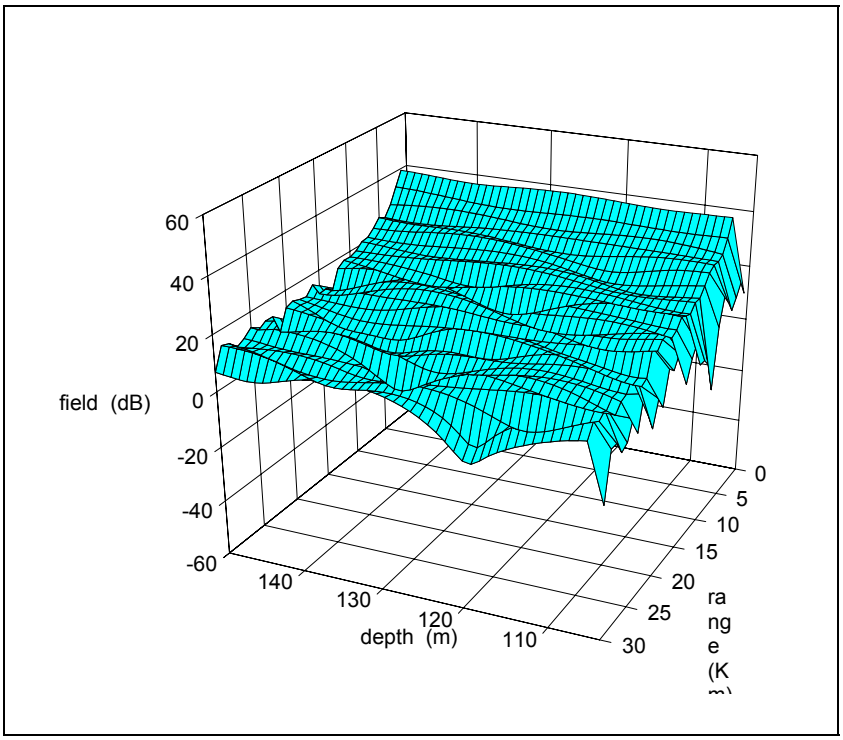

Figure 8. Acoustic field in the source layer for a transmission frequency of 10 Hz.

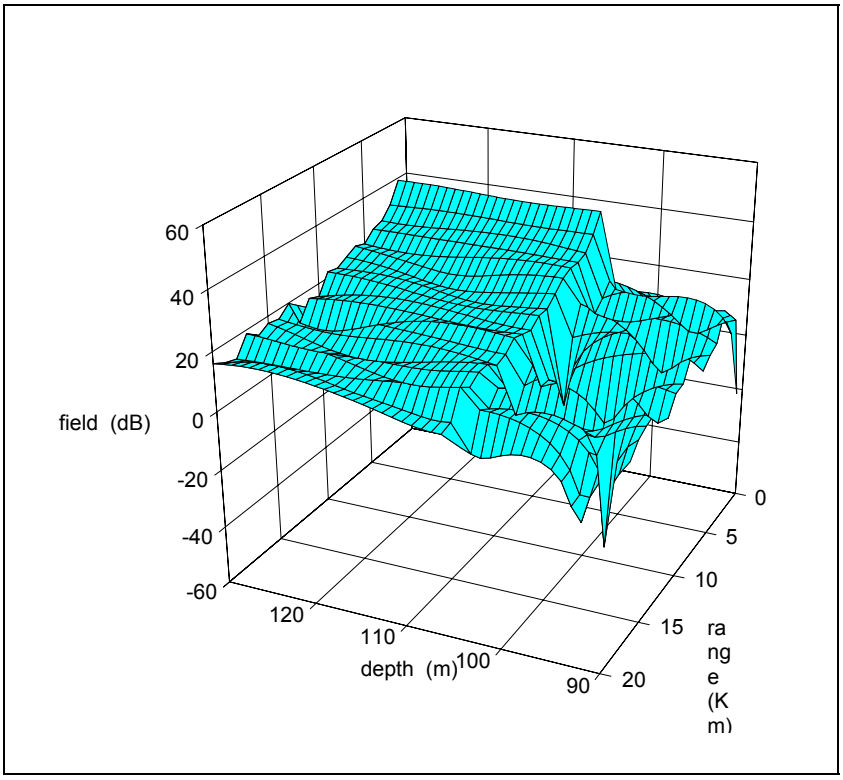

Figure 9. Acoustic field at the separation layer between source layer and the next layer for a frequency of 10 Hz.

In figure 10 the disturbance in the acoustic field is presented versus frequency when the receiver is within the source layer and in a distance of 50 km from the source. The same situation, but for a distance of 200 km is presented in figure 11.

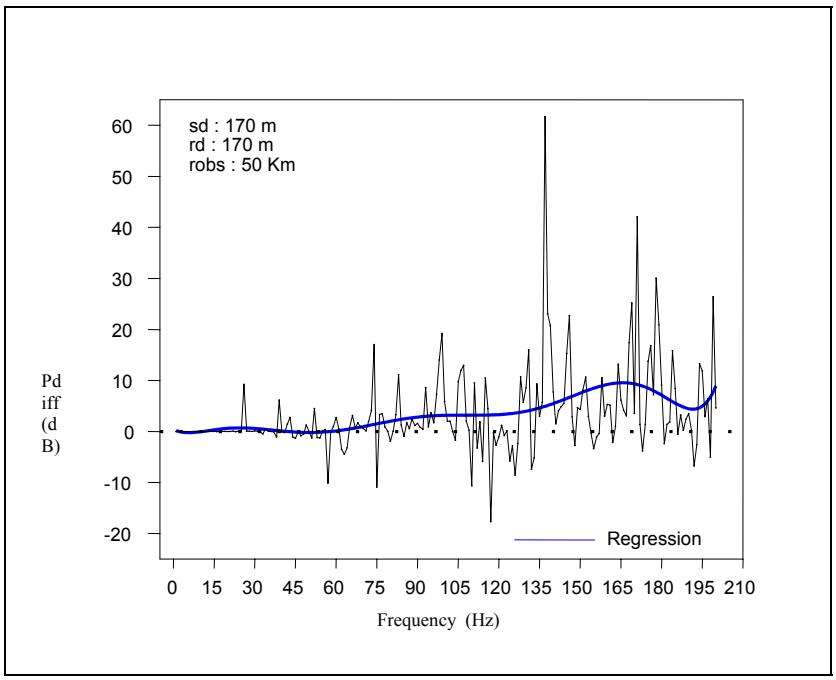

Figure 10. Acoustic field variation with respect to the frequency when the receiver's distance from the source is 50 km and is positioned at the same layer with it.

From figures 10 and 11 it is clear that the disturbance in the acoustic field in increasing with frequency while the same is true also with the distance of the receiver from the source. The later can be explained from the fact that as the distance is increasing the effect of the primary field to the total field is decreasing and the disturbances at the secondary fields are becoming more important for the acoustic field. Another interesting remark has to do with the existence of some frequencies within the range of 0-200 Hz were a kind of resonance is noticed resulting in larger disturbances for the acoustic field.

Figure 12 presents the disturbance of the acoustic field versus the distance of the receiver from the source for a frequency of 150 Hz. The most interesting remark here, except of course from the expected increase of the disturbance with the distance, has to do with the presence of a periodic variation of the disturbance with the distance. This phenomenon may be a result of the usage of a periodic function for the description of the medium disturbance.

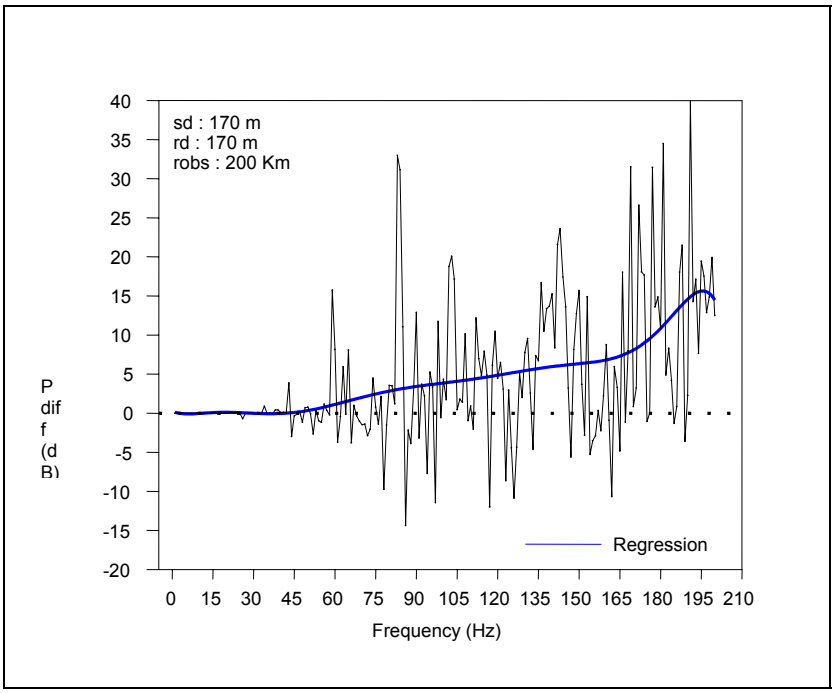

Figure 11. Acoustic field variation with respect to the frequency when the receiver's distance from the source is 200 km and is positioned at the same layer with it.

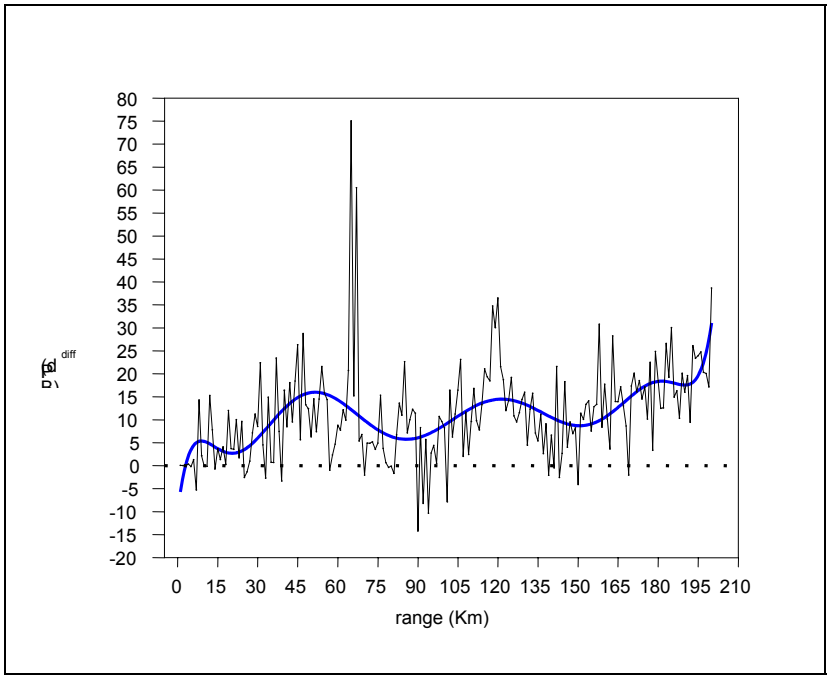

Figure 12. Acoustic field variation with respect to the source receiver distance for a frequency of 150 Hz

Finally this group of results will be concluded with figure 13 were the acoustic field with the disturbance is presented. What is really interesting in this figure is the diffusion of the acoustic energy within the different layers because of the presence of the medium disturbance. The difference becomes more clear If we compare this figure with figure 9 were the difference in the acoustic field from the source layer to the next layer is much more clear than in the case of figure 13.

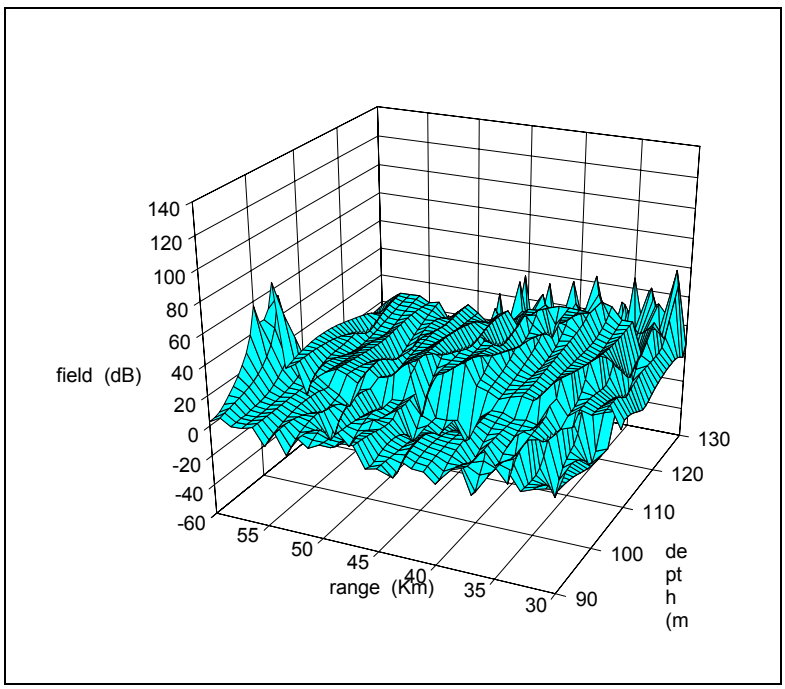

Figure 13. Acoustic field at the surface between the source layer and the next layer at a frequency of 70Hz.

6. CONCLUSIONS

An efficient method to calculate acoustic waves propagation has been developed for horizontally layered mediums as well as for horizontally varying medium. The method provides a tractable transfer function for the sea propagation medium permitting a transfer function description that could be easily used for signal source estimation and identification. At the same time the effects of inhomogeneities of the propagation medium are examined through numerical results which show significant alterations of the acoustic field.

REFERENCES

[1] Rubano L.A., "Acoustic Propagation in Shallow Water over a Low Velocity Bottom", J. Acoust. Soc., Am. 67, 1608-1613, 1980.

[2] Lo, En-Cen, Zhou, Ji-Xun, Chang Er-Chang, "Normal Mode Filtering in Shallow Water", J. Acoust. Soc., Am. 74, 1833, 1983.

[3] Boyles C.A., Acoustic Waveguides. Applications to Oceanic Sciences, John Willey, 1984.

[4] Kong J.A., Electromagnetic Wave Theory, Wiley, New York, 1986.

[5] Jensen F.B., Kuperman W.A., Porterand M.B. and Schmidt H., Computational Ocean Acoustics,AIP Press, New York, USA, 1994.

[6] Siegmann W.L., Kriegsmann G.A., Lee D., "A Wide-Angle Three-Dimensional Parabolic Equation", J. Acoust. Soc., Am. 78, 659-664, 1985.

[7] Noble B., Methods Based on the Wiener-Hopf Technique, Pergamon Press, New York, 1958.

[8] Mittra R. and Lee S.W., Analytical Techniques in the Theory of Guided Waves, McMillan Co., New York, 1971.

[9] A.J.Amditis, N.K. Uzunoglu, "An Efficient Method for Calculation of the Acoustic Field in a Horizontally Varying Stratified Sea" pp. 267-272 of the proceedings of the 3rd EUROPEAN CONFERENCE ON UNDERWATER ACOUSTICS, HERACLION, CRETE, GREECE, 24-28 JUNE 1996.

[10] Spofford C.W., Garon H.M., " Deterministic Methods of Sound-Field Computation", in "Oceanic Acoustic Modelling", SACLANTCEN Conference Proceedings, CP-17, Part 7, SACLANTCEN, La Spezia, Italy, 1975.

[11] Newton R.G., Scattering Theory of Waves and Particles, 2nd ed., Springer-Verlag, New York, 1982.

[12] Abramowitz M. and Stegun I.A., Handbook of Mathematical Functions, Dover, New York, 1970.

[13] Erdelyi A., Asymptotic Expansions, Dover Publications INC., New York, 1956.

[14] Davis P.J. and Rabinowitz P., Methods of numerical integration, Academic Press, 1975.

[15] Elter P.C., Underwater Acoustic Modelling, Elsevier, Amsterdam, The Netherlands, 1991.

[16] Amditis A., Uzunoglu N., "Computation of Acoustic Wave Propagation in Random Sea Media Using Integral Equations", AP-S/URCI Conference, Atlanta, USA ,1998.

[17] Jensen F.B., "Numerical Models in Underwater Acoustics", Hybrid Formulation of Wave Propagation and Scattering, edited by L.B. Felsen, Martinus Nijhoff Publishers, Dordrecht, Holland, 1984, also in SACLANTCEN, Report SR-83, SACLANTCEN, La Spezia, Italy, 1984.

[18] Williams A.O., "Discrete, Continuous and Virtual Modes in Underwater Sound Propagation", ALR-TR-76-40, Applied Research Laboratory, Austin, Texas, 1976.

[19] DiNapoli F.R., Deavenport R.L., "Theoretical and Numerical Green's Function Field Solution in a Plane Multilayered Medium", J. Acoust. Soc., Am. 67, 92-105, 1980.

[20] Li S. and Schultheiss P.M., "Depth measurement of remote sources using multipath propagation", IEEE J. Oceanic Eng., vol. 18, Oct. 1993.